Promoted Chondrogenesis of Cocultured Chondrocytes and Mesenchymal Stem Cells under Hypoxia Using In-situ Forming Degradable Hydrogel Scaffolds
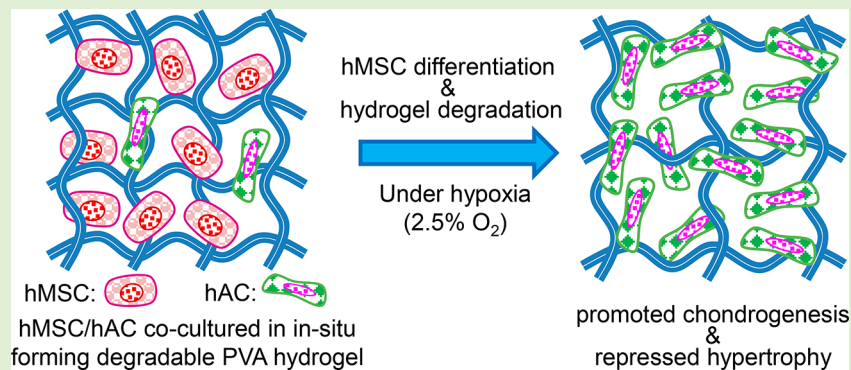
Xiaobin Huang,[†,‡] Yong Hou,[‡,§] LeiLei Zhong,[†] Dechun Huang,*[,∥] Hongliang Qian,[∥] Marcel Karperien,[†] and Wei Chen*[,§,∥]

[†]Department of Developmental BioEngineering, MIRA-Institute for Biomedical Technology and Technical Medicine, Faculty of Science and Technology, University of Twente, P.O. Box 217, 7500 AE Enschede, The Netherlands

[∥]Department of Pharmaceutical Engineering, School of Engineering, China Pharmaceutical University, Nanjing 210009, People's Republic of China

[§]Institute of Chemistry and Biochemistry, Freie Universität Berlin, Takustrasse 3, Berlin 14195, Germany

Ⓢ *Supporting Information*

hMSC differentiation & hydrogel degradation

Under hypoxia (2.5% O_2)

hMSC: hAC:

hMSC/hAC co-cultured in in-situ forming degradable PVA hydrogel

promoted chondrogenesis & repressed hypertrophy

ABSTRACT: We investigated the effects of different oxygen tension (21% and 2.5% O_2) on the chondrogenesis of different cell systems cultured in pH-degradable PVA hydrogels, including human articular chondrocytes (hACs), human mesenchymal stem cells (hMSCs), and their cocultures with a hAC/hMSC ratio of 20/80. These hydrogels were prepared with vinyl ether acrylate-functionalized PVA (PVA-VEA) and thiolated PVA-VEA (PVA-VEA-SH) via Michael-type addition reaction. The rheology tests determined the gelation of the hydrogels was controlled within 2−7 min, dependent on the polymer concentrations. The different cell systems were cultured in the hydrogel scaffolds for 5 weeks, and the safranin O and GAG assay showed that hypoxia (2.5% O_2) greatly promoted the cartilage matrix production with an order of hAC > hAC/hMSC > hMSC. The real time quantitative PCR (RT-PCR) revealed that the hMSC group exhibited the highest hypertrophic marker gene expression (COL10A1, ALPL, MMP13) as well as the dedifferentiated marker gene expression (COL1A1) under normoxia conditions (21% O_2), while these expressions were greatly inhibited by coculturing with a 20% amount of hACs and significantly further repressed under hypoxia conditions, which was comparative to the sole hAC group. The enzyme-linked immunosorbent assay (ELISA) also showed that coculture of hMSC/hAC greatly reduced the catabolic gene expression of MMP1 and MMP3 compared with the hMSC group. It is obvious that the hypoxia conditions promoted the chondrogenesis of hMSC by adding a small amount of hACs, and also effectively inhibited their hypotrophy. We are convinced that coculture of hAC/hMSC using in situ forming hydrogel scaffolds is a promising approach to producing cell source for cartilage engineering without the huge needs of primary chondrocyte harvest and expansion.

■ INTRODUCTION

Articular cartilage, a connective tissue in the knee joint of humankind, provides mechanical support for the joints and responsible for the smooth joint movement.[1−3] The main matrix of cartilage includes collagens and proteoglycans with the compressive and tensile properties. Osteoarthritis (OA) is one kind of universal chronic joint disease with progressive degradation of joint matrix, and millions of people suffer from a lot of pain and inconvenient movement.[4−6] Due to its avascular

and neural properties, cartilage has limited self-repairing ability once it is irreparably damaged.

Articular chondrocytes (ACs) are a unique cell type with a low amount residing in the articular cartilages and producing the matrix of collagens and proteoglycans to maintain the

cartilage homeostasis.[7,8] It has been shown that autologous chondrocyte implantation (ACI) is a very promising method to treat the OA problem, since the adequate healthy ACs could produce the tissue matrix and recover the biofunctions.[9−11] However, it is highly limited by the donor-site morbidity and the dedifferentiation of isolated chondrocyte during proliferation in vitro. The common way to collect a sufficient amount of ACs for ACI requirement is to expand cells in vitro in monolayer, which could possibly lead to the dedifferentiation of ACs, resulting in useless fibrocartilage instead of hyaline cartilage after transplanting.[12] Mesenchymal stem cells (MSCs), which are often isolated from the bone marrow, are found to own the ability of differentiation to chondrogenic lineages after expanding in vitro and considered as suitable candidates for the promotion of cartilage regeneration.[13−16] However, the problems of their hypotrophy and subsequent endochondral ossification always come out after implantation.[17,18] It is reported that the coculture of MSCs and ACs could improve the chondrogenesis and suppress the hypertrophic development in MSCs, in which the proliferation of chondrocyte was also enhanced by the presence of MSCs, together with the significant chondrogenic differentiation of MSCs triggered by chondrocytes.[19−23] It is indicating that the coculture system using MSCs and ACs not only benefits for the chondrogenesis process, but also reduces the amount of ACs which is required for the ACI treatment.

ACs have been shown to be well adapted to the low oxygen conditions and capable of maintaining the energy metabolism mainly through the glycolytic pathway, because they are embedded in an extensive extracellular matrix and exposed to a concentration of approximately 6% O_2 in the superficial layer, as well as the calcified layer with the O_2 concentration less than 1%.[24,25] Hypoxia is considered as a positive influence on the healthy ACs phenotype and cartilage matrix formation, which can also promote the differentiation of MSCs toward chondrogenic lineage, and the restoration of chondrogenic phenotype in passaged ACs. Meretoja et al. cocultured bovine ACs and MSCs with a ratio of 30/70 using electrospinning PCL microfiber mats under a low oxygen tension (5% O_2) and demonstrated the enhancement of cartilaginous matrix production under hypoxia and inhibition of MSC hypertrophy by cocultured systems.[26]

Hydrogels have been a very attractive class of cell scaffolds with 3D hydrophilic networks and excellent water uptake capacity, which are highly suitable for cartilage regeneration.[27−32] Hydrogel scaffolds could provide a promising mimicking cell matrix for enhanced chondrogenic differentiation of MSCs and redifferentiation of ACs, increasing cartilage matrix production and improving cartilage repair.[33−37] Burnsed et al. cultured MSCs using the shark and pig cartilage extracellular matrix (ECM) hydrogels and realized enhanced chondrocytic differentiation of MSCs without exogenous growth factors.[38] Rackwitz et al. used agarose hydrogels to separately culture MSCs and chondrocyte and found that MSCs underwent sustained chondrogenic differentiation and exhibited superior matrix deposition and integration with the pretreatment of transforming growth factor-beta 3 (TGF-β3) as compared to dedifferentiated chondrocytes under the same conditions.[39] Zhu et al. demonstrated that hypoxia promoted MSC chondrogenesis and suppressed subsequent hypertrophy using photo-cross-linked hyaluronic acid (HA) hydrogels.[40] To the best of our knowledge, there have been few reports about a chondrogenesis study in coculture systems of MSCs and ACs

under hypoxic conditions using in situ forming degradable hydrogels. In the present study, we coencapsulated hMSCs/ hACs with a ratio of 80/20 using pH-degradable PVA hydrogels, which can be injected and solidified in situ, to investigate the effects of hypoxia (2.5% O_2, close to the natural oxygen level of chondrocyte in vivo) on the cell chondrogenesis and the inhibition of dedifferentiation and hypotrophy with the treatment of TGF-β3 and dexamethasone. Besides the detection of the cartilage markers and hypertrophic markers, we also investigated the catabolic markers that could more comprehensively demonstrate the chondrogenesis. We considered all the favorable factors, including human cell source, coculture system, natural hypoxia condition, injectable degradable hydrogel scaffolds, and cytokines, to find an optimal cell source for cartilage regeneration.

■ MATERIALS AND METHODS

Materials. Ethylene glycol vinyl ether (Aldrich, 97%), acryloyl chloride (Aldrich, 97%), triethylamine (Et$_3$N, Acros, 99%), 2,2′-(ethylenedioxy)diethanethiol (Sigma, 95%), and p-toluenesulfonic acid monohydrate (PTSA, Sigma-Aldrich, 98%) were used as received. Poly(vinyl alcohol) (PVA, Mowiol 3−85, M_w = 16000 g/mol) was kindly provided from Kuraray Europe GmbH (Germany). Vinyl ether acrylate (VEA) and VEA-functionalized PVA (PVA-VEA) were synthesized according to our previous report,[41] in which the degree of VEA functionality on PVA-VEA was determined as 4.0% by ^{1}H NMR. Thiolated PVA-VEA (PVA-VEA-SH) was prepared by dropwise addition of PVA-VEA in methanol (25.0 mg/mL) into 2,2′-(ethylenedioxy)diethanethiol of methanol solution (3.0 mmol, 75 equiv to VEA units) in the presence of a catalytic amount of Et$_3$N under a nitrogen atmosphere for 24 h (Figure S1).

^{1}H NMR spectra were recorded on a Bruker ECX 400. The chemical shifts were calibrated against residual solvent peaks as the internal standard. SEM images were performed on a Hitachi scanning electron microscope (SU8030). The rheological studies were measured by a Kinexus lab rheometer (Malvern) using a parallel plate with 40 mm diameter in single frequency model.

Hydrogel Formation. Hydrogel samples were prepared with a mixture of PVA-VEA and PVA-VEA-SH at room temperature via Michael-type addition reaction. In a typical example, PVA-VEA and PVA-VEA-SH were separately dissolved in phosphate saline buffer (PBS, pH 7.4) with a concentration of 100 mg/mL at 4 °C and then mixed with a volume ratio of 1/1 to form hydrogels quickly in minutes by slight shaking at room temperature.

Gel Content and Water Uptake Test. To determine the gel content, PVA-VEA (0.10 g) and PVA-VEA-SH (0.10 g) were used to prepared hydrogels as above-mentioned. After that, the hydrogels were immersed in water/methanol to remove unreacted polymer. Gel content was determined gravimetrically by the formulation of W_d/W_0 × 100%, in which W_d was the weight of dry gel after lyophilizing and W_0 was the initial polymer weight of PVA-VEA and PVA-VEA-SH for the hydrogel preparation.

The dry hydrogels (W_d) after lyophilizing were immersed in Milli-Q water at 37 °C to reach the swelling equilibrium, and then the swollen samples were taken out from water and dried by removing the surface water with filter paper. The swollen samples were weighted as W_s. The water uptake of hydrogels was determined by the formulation of (W_s − W_d)/W_d × 100%.

Rheological Characterization. To study the mechanical properties of the hydrogels, storage modulus (G') and loss modulus (G'') were measured by a Kinexus lab rheometer (Malvern) using a parallel plate with a 40 mm diameter in single frequency model. In a typical example, 0.25 mL of PVA-VEA and PVA-VEA-SH were mixed and quickly loaded on the bottom platform, and the tests were performed immediately. Measurements were conducted at room temperature with a frequency of 0.5 Hz and a constant 0.1% strain in triplicate. The mesh size (ξ) of the network, that is, the spacing of the effective elastic units can be estimated from the formulation:[42]
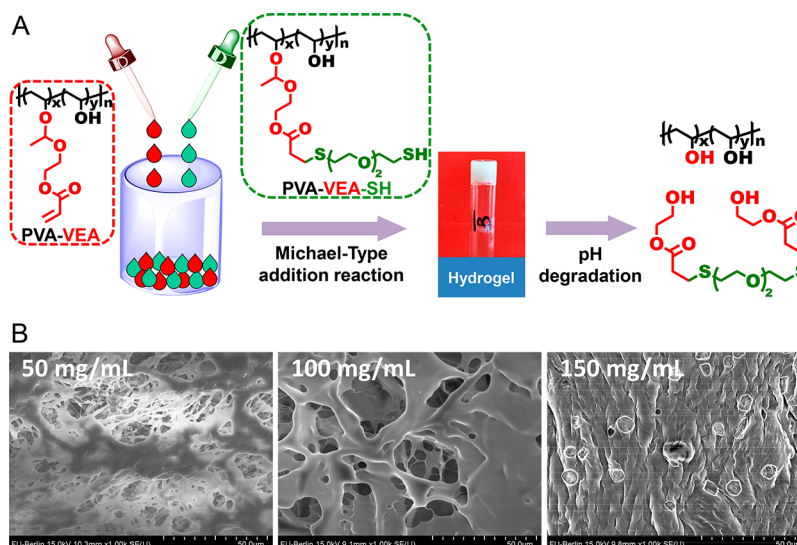
Figure 1. (A) Illustration of pH-degradable PVA hydrogels formed by Michael-type addition reaction and pH-degradation to PVA itself; (B) SEM images of PVA hydrogels formed with polymer concentrations of 50, 100, and 150 mg/mL.

$$\xi = \left(\frac{G'_{\infty} N_A}{RT} \right)^{-1/3}$$

where G'_{∞} is the final steady state elastic modulus, R is the gas constant, and T is the absolute temperature.

Degradation Characterization. The studies of hydrogel degradation were performed in phosphate saline buffer (PBS, pH 7.4 and pH 6.5) at 37 °C by weight loss (%) of the hydrogels. In a typical example, hydrogel samples were immersed in 2 mL of PBS, and the weight of the hydrogels was determined as W_{t0}. At regular time intervals, samples were taken out from the buffer and dried with filter paper to remove the surface water, and the weight of the hydrogels was determined as W_t. The degradation percentage was calculated as $W_t/W_{t0} \times 100\%$. The experiments were performed in triplicate.

Cell Harvest and Expansion. Human primary chondrocytes were derived from healthy looking and full thickness cartilage and dissected from knee biopsies of three patients (age: 60 ± 3 years) undergoing total knee replacement, according to a previous report.[43] To isolate the cells, the cartilage was digested in chondrocyte proliferation medium containing collagenase type II (0.15% Worthington, NJ, U.S.A.) for 20−22 h. Subsequently, the hACs were expanded at a density of 3000 cells/cm² in chondrocyte proliferation medium until the monolayer reached 80% confluency. Chondrocyte proliferation medium was consisted of DMEM supplemented with 10% fetal bovine serum (FBS), 1× nonessential amino acids, ascorbic acid 2-phosphate (0.2 mM, AsAP), proline (0.4 mM), penicillin (100 U/mL), and streptomycin (100 µg/mL). The hMSCs were isolated from human bone marrow aspirates and cultured in MSCs proliferation medium (α-MEM) supplemented with 10% FBS, 1% L-glutamax, ascorbic acid (0.2 mM), penicillin (100 U/mL), streptomycin (100 µg/mL), and basic fibroblast growth factor (bFGF, 1 ng/mL).

Cell Seeding and Chondrogenic Culture. PVA-VEA and PVA-VEA-SH were dissolved in DMEM medium at a concentration of 200 and 100 mg/mL at 4 °C, respectively. hMSCs, hACs and their combination (hMSCs/hAC: 80/20) were first mixed with PVA-VEA solution at a cell density of 5 million (M)/mL, respectively, resulting in a final PVA-VEA concentration of 100 mg/mL. The mixtures of cells and PVA-VEA were added into 96-well plate (50 µL per well), and then another 50 µL of PVA-VEA-SH solution was added into the well to mix with the cells and PVA-VEA by slight shaking. The hydrogels entrapped with cells formed quickly after the addition of PVA-VEA-SH. The cell-embedded hydrogel systems were incubated in 100 µL of chondrogenic differentiation medium (DMEM supplemented with 50 µg/mL of insulin−transferrin−selenium (ITS) premix, 50 µg/mL of AsAP, 100 µg/mL of sodium pyruvate, 10 ng/

mL of TGF-β3, 10^{-7} M of dexamethasone (DEX), 100 U/mL of penicillin and 100 µg/mL of streptomycin), under 21% O_2 (normoxia) or 2.5% O_2 (hypoxia) for a period of 5 weeks. The medium was refreshed twice per week.

RNA Extraction and Quantitative Polymerase Chain Reaction (qPCR). RNAs were isolated from cell-encapsulated hydrogels after crashing using the Trizol reagent (Thermo Fisher Scientific). The concentration and purity of RNA samples were determined by Nanodrop 2000 (Thermo scientific). mRNAs were reverse-transcribed into cDNAs using iScript cDNA Synthesis kit (Bio-Rad). qPCR was performed on the SYBR Green sensimix (Bioline) to measure the gene expression of cartilage markers collagen type II (COL2A1) and aggrecan (ACAN), dedifferentiation marker collagen type I (COL1A1), hypertrophic markers collagen type X (COL10A1) and alkaline phosphatase (ALPL), catabolic genes matrix metalloproteinase (MMP 1 and 3). PCR reactions were carried out using the Bio-Rad CFX96 (Bio-Rad) under the following conditions: cDNAs were denatured at 95 °C for 5 min, followed by 39 cycles of 95 °C for 15 s, 60 °C for 15 s, and 72 °C for 30 s. The melting curve was generated for testing each reaction of primer dimer formation and nonspecific priming. Gene expression was normalized using RPL13A and expressed as fold induction compared with controls.

Safranin O Staining. Samples were fixed with 10% formalin phosphate buffer (PB, pH 7.0) for 1 h at room temperature. After embedding in cryomatrix and freezing, the samples were cut into slices with the thickness of 7 µm by cryotome (Shandon). The slices were stained with a 0.1% safranin O (Sigma-Aldrich) solution for 5 min for sulfated glycosaminoglycans (GAG) observation, and then counterstained with hematoxylin (Sigma-Aldrich) to visualize nuclei. All the samples imaged by Nanozoomer (Iwata City, Japan).

Immunofluorescent Staining. Samples were preincubated with 5.0 µg/mL of proteinase K (Sigma-Aldrich) at room temperature for 10 min, followed with 1 mg/mL of hyaluronidase (Sigma-Aldrich) at 37 °C for 40 min. The collage type II was blocked by rabbit antihuman collagen II antibody (ab34712, Abcam) in 5% BSA PBS solution for 1 h, and diluted 100-fold with 5% BSA PBS at 4 °C. After 12 h, AlexaFluor 546-labeled goat antirabbit antibody in 5% BSA PBS solution was added to incubate for another 2 h at room temperature. Samples were rinsed with PBS in each step. Mounting medium with DAPI was added and images were visualized by BD pathway confocal microscopy.

Enzyme-Linked Immunosorbent Assay (ELISA). The culture medium was respectively collected at week 1, week 3 and week 5. The secreted MMP1 in medium was measured by ELISA using mouse antihuman MMP1 antibody (MAB901-SP, R&D systems), followed by
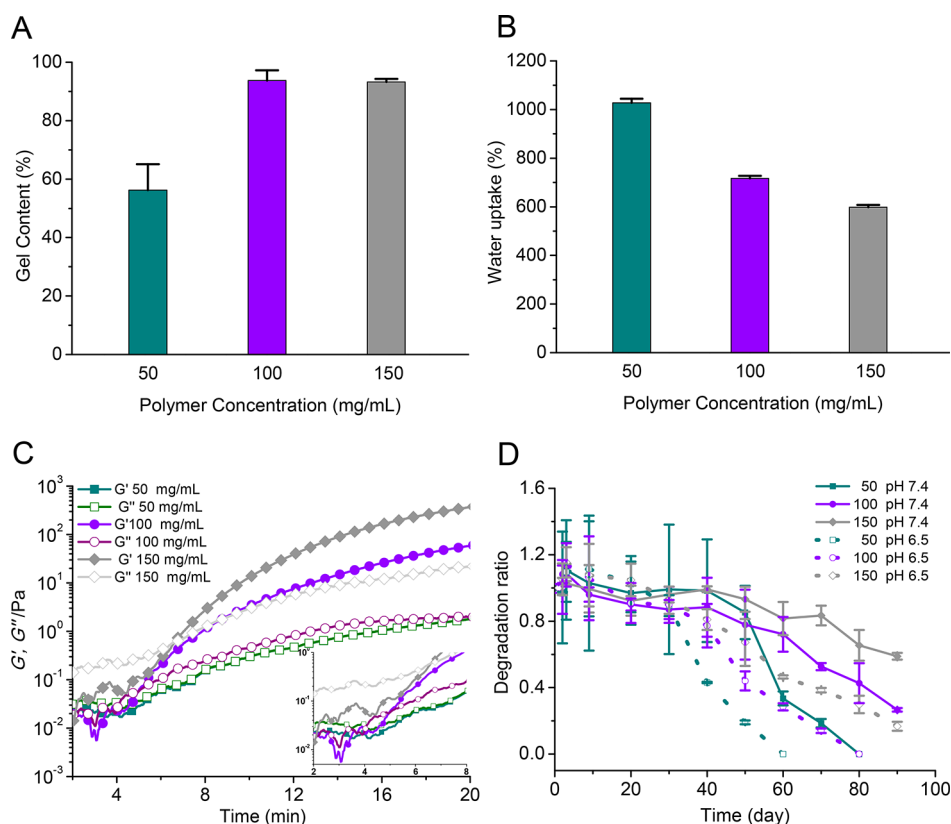
Figure 2. Gel content (A) and water uptake (B) of PVA hydrogel formed in PBS buffer (pH 7.4) at room temperature with polymer concentrations of 50, 100, and 150 mg/mL; (C) Storage modulus (G') and loss modulus (G'') of PVA hydrogels as a function of time determined by rheology test (inlet: enlarged view during the first 8 min); (D) Swelling and degradation behavior of PVA hydrogels performed in PBS with different pH (pH 7.4 and 6.5).

incubation with a peroxidase-linked rabbit antimouse antibody. The amount of horseradish peroxidase (HRP) was quantified by the addition of tetramethylbenzidine (TMB, 1-Step Ultra TMB-ELISA, Thermo Scientific) and measured at an absorption wavelength of 450 nm (Micro Plate Reader). The results were expressed as relative production by comparing with the control group of hMSC under normoxia.

GAG and DNA Assay. In order to measure the GAG concentration, samples were predigested in 250 uL of Tris-HCl buffer (0.05 M Tris, 1 mM $CaCl_2$, pH 8.0) containing proteinase K (1 mg/mL, Roche) at 56 °C for 16 h. Diluted samples (25 μL) were mixed with 150 μL of 1,9-dimethylmethylene blue (DMMB)-dye aqueous solution (DMMB, 20.0 mg/L; glycine, 3.04 g/L; NaCl, 2.38 g/L). The measurement was performed by Micro Plate Reader at an absorption wavelength of 525 nm. Relative cell number was determined by quantifying total DNA amount using a QuantiFluor dsDNA System kit (Promega) according to the manufacturer's instructions.

ALP Assay. To evaluate alkaline phosphatase (ALP) activity, samples were washed with PBS and lysed with CDPStar lysis buffer (Roche). Cell lysate was added into CDPStar reagent (Roche), and luminescence was measured using Vector Microplate Luminometer (Promega). The luminescence units were corrected for DNA content.

Statistical Analysis. Each experiment was performed in triplicate. Statistical differences between two groups were analyzed by two-tailed student's t tests or one-way ANOVA. $P < 0.05$ was considered statistically significant. Data are expressed as the mean ± standard deviations (SD).

■ RESULTS AND DISCUSSION

Preparation and Characterization of PVA Hydrogels. PVA has a brilliant history of biomedical applications, specifically for the PVA-based hydrogels, which have been recognized as promising biomaterials and excellent candidates for tissue engineering applications. However, due to some disadvantages (i.e., degradation property), it requires further modification for desired and targeted applications. Here, we prepared pH-degradable VEA-functionalized PVA (PVA-VEA) and thiolated PVA-VEA (PVA-VEA-SH), which were successfully used for in situ forming PVA hydrogels by mixing PVA-VEA and PVA-VEA-SH via Michael-Type addition reaction in minutes (Figure 1A). Fast gelation is highly preferred for in situ forming hydrogels; otherwise, it may cause diffusion of hydrogel precursors or bioactive molecules into the surrounding areas in vivo and even induce the failure of the gel formation. Michael-type addition reaction between thiolated polymers and vinylsulfone or acrylate functionalized polymer has been considered as an efficient and green chemistry method for the orthogonal hydrogels preparation under physiological conditions without any catalyst.[44,45] It is interesting that here the degradation products of hydrogels are still PVA itself and nontoxic diethylene glycol derivative. The SEM images showed that, as the polymer concentration increased from 50 to 150 mg/mL, the porous structures of hydrogels became more sophisticated (Figure 1B). The mesh sizes of hydrogel networks were further calculated according to the final steady state elastic modulus (G'_{∞}), which showed a decrease from 37 to 19 nm (Figure S2), being in good line with the SEM observation.

The gel content and water uptake of PVA hydrogels prepared with different concentrations were investigated by gravimetrical method. The gel content increased from 56.2% to 93.2% as the PVA concentrations ranged from 50 to 150 mg/mL (Figure 2A), while the water uptake showed a gradually decrease from
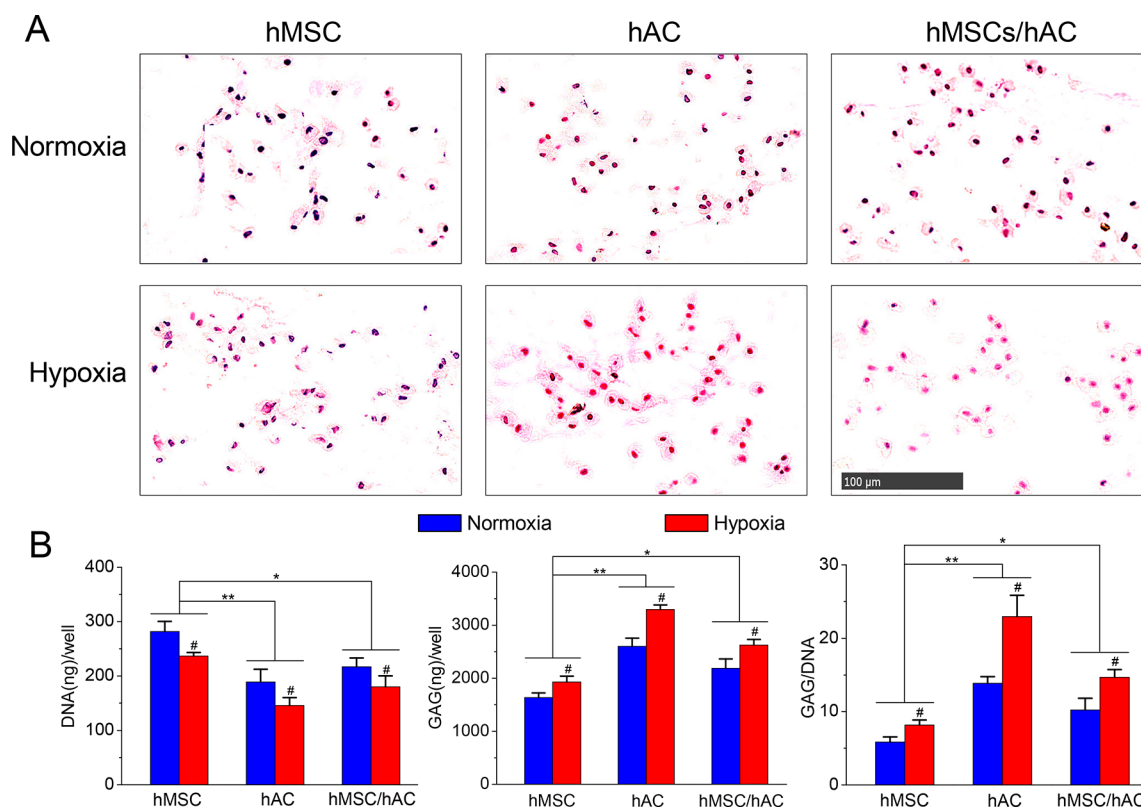
Figure 3. (A) Safranin O staining for GAG production under normoxia and hypoxia conditions after five-week incubation (cell nuclei stained by hematoxylin, scale bar = 100 μm); (B) Quantitative detection of DNA and GAG after five-week incubation by biochemical assay. The cells (hMSC, hAC, and hMSC/hAC) were cultured in PVA hydrogels in the chondrogenic differentiation medium under normoxia and hypoxia conditions. Data were expressed as the mean ± standard deviations (SD, "#" represents the significant difference between normoxia and hypoxia, *$p < 0.05$, and **$p < 0.01$).

1030% to 600% (Figure 2B), which could be attributed to higher cross-linking efficiency and cross-linking density induced by the increased polymer concentrations. It was also in line with the morphology observation of SEM images that the network perfection was performed at higher polymer concentration (Figure 1B).

The mechanical properties of PVA hydrogel samples were further studied by rheology test at room temperature. The kinetics of gel formation was followed by monitoring the storage modulus (G') and loss modulus (G'') in time (Figure 2C). The crossover point of G' and G'' is defined as gel point. It was found that although the gelation would occur at a concentration of 50 mg/mL, the storage modulus G' was relatively low (1.7 Pa) and the hydrogels were too soft. As the polymer concentration increased to 100 mg/mL, the storage modulus G' reached 60 Pa with gelation time less than 5 min. The storage modulus G' of the hydrogels could even go higher (370 Pa) at a polymer concentration of 150 mg/mL; however, the gelation became slow, and the swelling ratio and water uptake of hydrogels were much lower. The polymer concentration also affected the degradation behavior of PVA hydrogels at physiological conditions or in the mimicking inflammatory pH environments (pH 6.5). All the PVA hydrogels showed overall slow degradation during the first 20 days (Figure 2D). However, the hydrogel degradation became much fast at pH 6.5, in which the degradation time of 50% swelling ratio was 38, 49, and 60 days for the polymer concentrations of 50, 100, and 150 mg/mL, respectively. The gel degradation would provide space for cell stretching and

proliferation, especially for the synthetic hydrogels with the pore size much smaller than mammalian cells.[46] In our preliminary test, we found that the proliferation of cells was highly inhibited in the hydrogels at a concentration of 150 mg/mL, probably due to the limited space and insufficient exchange of oxygen, nutrient and waste across the hydrogels with such high cross-linking density. The degradation of hydrogels with the concentration of 150 mg/mL showed much more slow at both pH 7.4 and 6.5. Considering the mechanical property, gelation time, and degradation behavior, PVA hydrogels formed with the concentration of 100 mg/mL were used for the following biological study.

GAG Production. The hydrogels showed excellent biocompatibility to culture hMSC, hAC, or hMSC/hAC with high cell viability detected by PrestoBlue assay after five-week incubation (Figure S3). The cell chondrogenesis was determined by analyzing gene and protein expression profiles and the matrix production of hMSC and hAC or hMSC/hAC groups under normoxia (21% O_2) and hypoxia (2.5% O_2) conditions for 5 weeks. There are plenty of studies indicate that chondrocytes may lose their differentiation phenotype and potential cartilage formation capability after expanding in vitro, which was reflected by the high expression of dedifferentiation COL1A1 marker.[47−49] Since hypoxia was reported to have the positive effects on the 3D chondrocyte redifferentiation,[50] hMSC and hAC are hypothesized to realize the differentiation or redifferentiation process in hydrogel scaffoldss with low oxygen level of 2.5%, mimicking the physiological oxygen tension conditions within the cartilage tissue. hMSC, hAC, and
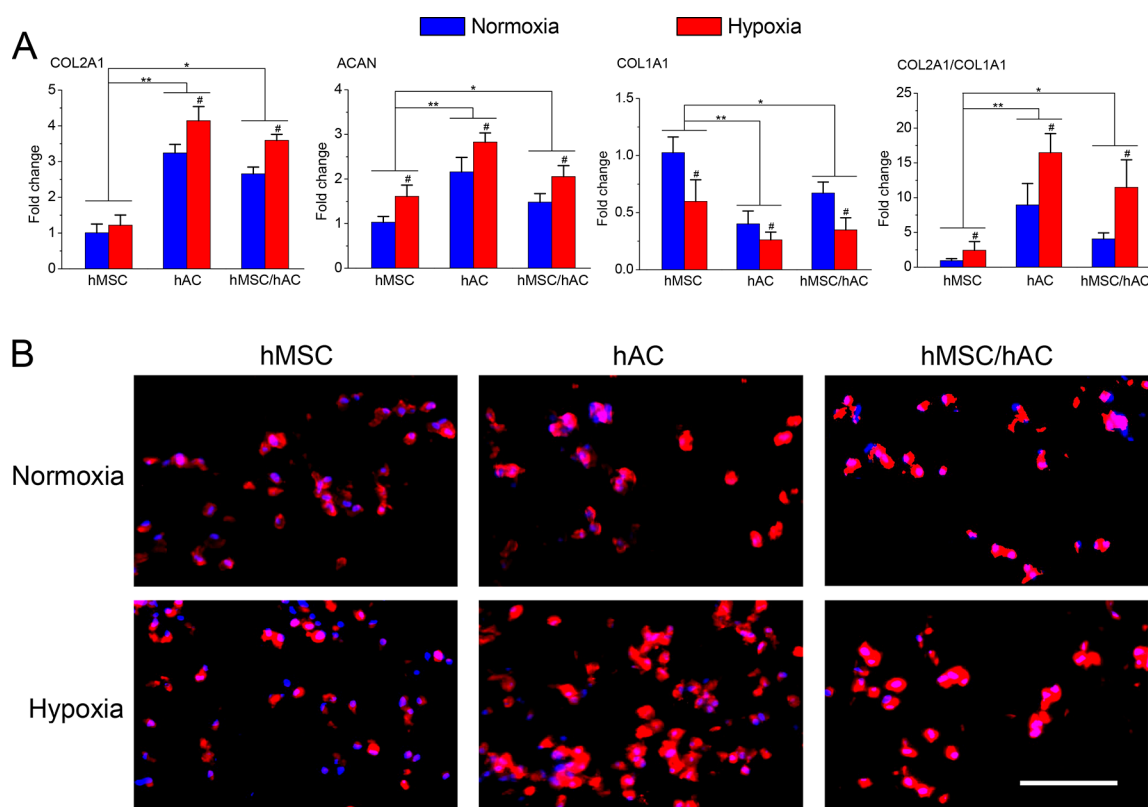
Figure 4. (A) Gene expressions of cartilage markers of COL2A1, ACAN, COL1A1, and COL2A1/COL1A1 after a five-week incubation measured by RT-PCR; (B) Deposition of collagen type II after five-week incubation detected by immunofluorescence staining. The cells (hMSC, hAC, and hMSC/hAC) were cultured in PVA hydrogels in the chondrogenic differentiation medium under normoxia and hypoxia conditions. For the immunofluorescence staining, the cells were first treated with mouse anticollagen type II antibody, followed by Alex 564-labeled antimouse second antibody, and the cell nuclei were stained with DAPI (scare bar = 200 μm). Data were expressed as the mean ± standard deviations (SD, "#" represents the significant difference between normoxia and hypoxia, *$p < 0.05$, and **$p < 0.01$).

their combination (hMSC/hAC: 80/20) were seeded in the porous hydrogel scaffolds and continuously cultured in chondrogenic medium for 5 weeks under hypoxia or normoxia conditions. The GAG production was detected by Safranin O staining and GAG assay. As expected, the Safranin O staining showed that hypoxia greatly promoted the GAG production in all cell types (Figure 3A), in which the groups of hAC and hMSC/hAC coculture exhibited slightly higher intensity than hMSC group under normoxia conditions, while much stronger staining presented under hypoxia conditions. The results of GAG assay was in line with the observation of Safranin O staining. Although the hMSC group showed the highest DNA content, the concentration of GAG in hAC and coculture groups was higher than that of hMSC under both of normoxia and hypoxia conditions (Figure 3B). After normalizing to DNA, the values of GAG/DNA in hAC and coculture groups were significantly higher than hMSC, especially that hAC group and cocultured group showed 2.8× and 1.8× higher than hMSC group under hypoxia conditions, respectively.

Cartilage Markers. In order to assess the expression of cartilage markers from the embedded cells in hydrogels under different O₂ tension, the gene expression of cartilage markers, COL2A1 and ACAN, and the dedifferentiation marker COL1A1 were measured by RT-PCR. Compared to the normoxia conditions, the expressions of COL2A1 and ACAN were significantly higher and COL1A1 was relatively lower under hypoxia conditions (Figure 4A). It should be also noted that the ratio of COL2A1/COL1A1 was much higher for hAC

and hMSC/hAC, especially under hypoxia conditions (hAC: 6.8×, hMSC/hAC: 4.7×), indicating their much better chondrogenic differentiation and redifferentiation degree. Furthermore, hAC and hMSC/HAC coculture groups showed the similar expression trend which had higher expression of COL2A1 and ACAN and lower COL1A1 expression as compared to the hMSC group under both normoxia and hypoxia conditions (Figure 4A). The protein level of collagen type II expression was detected by immunofluorescence, and hAC and hMSC/hAC groups exhibited much stronger positive staining than hMSC under hypoxia conditions, which was consistent with the gene expressions (Figure 4B). However, the positive matrix staining was hard to observe in the intercellular space, which might be due to the slow degradation of hydrogels that impeded the cartilage matrix deposition.[51,52] We also checked the expression of hypoxia-induced factor 1a (HIF1a) to confirm whether hypoxia could influence chondrogenesis via low oxygen related genes. As shown in Figure S4, HIF1a presented similar express trend with the cartilage markers COL2A1 and ACAN. However, the mechanism of hypoxia-induced enhanced chondrogenesis needs further investigations.

Catabolic and Hypotrophic Markers. The main issue in the cell based articular cartilage repair is that the dedifferentiation and hypotrophy of hAC and hMSC-differentiated chondrocytes commonly result in the formation of fibrocartilaginous instead of hyaline cartilage,[12] or endochondral ossification after implantation.[1,18,19,53] Therefore, it is extremely important to inhibit the dedifferentiation and hypertrophy in
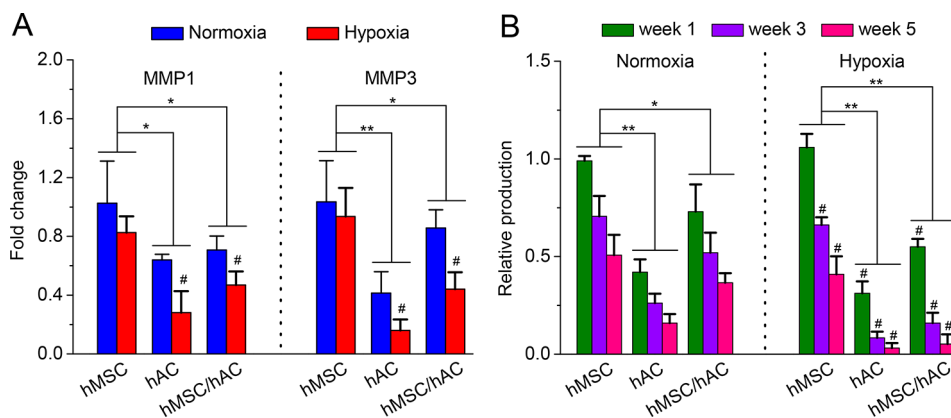
Figure 5. (A) Gene expressions of catabolic genes of MMP1 and MMP3 after five-week incubation detected by qPCR; (B) Secreted MMP1 protein quantified by ELISA at weeks 1, 3, and 5. The cells (hMSC, hAC, and hMSC/hAC) were cultured in PVA hydrogels in the chondrogenic differentiation medium under normoxia and hypoxia conditions. Data were expressed as the mean ± standard deviations (SD, "#" represents the significant difference between normoxia and hypoxia, *$p < 0.05$, and **$p < 0.01$).
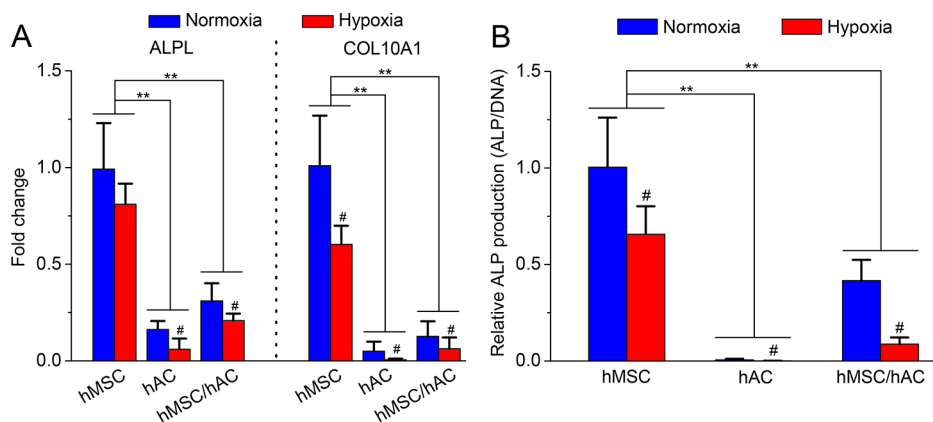

Figure 6. (A) Gene expressions of hypertrophic markers of ALPL and COL10A1 after a five-week incubation detected by qPCR; (B) Relative ALP production measured by ALP assay. The ALP activity was expressed as relative production by normalizing to the total DNA amount. Data were expressed as the mean ± standard deviations (SD, "#" represents the significant difference between normoxia and hypoxia, *$p < 0.05$, and **$p < 0.01$).

cell-based human osteoarthritis treatment. Cartilage extracellular matrix degradation is a typical feature in cartilage degradation diseases like osteoarthritis, and MMPs play a vital role in the process. Here, the gene expression of catabolic genes such as MMP1, MMP3 was measured by RT-PCR, and the protein level of secreted MMP1 was detected by ELISA at weeks 1, 3, and 5. Compared to normoxia conditions, the expressions of MMP1 and MMP3 were relatively lower in hAC and coculture groups under hypoxia conditions (Figure 5B), while there was no obvious change in the hMSC group. It should be noted that much lower expressions of MMP1 and MMP3 were found in both hAC and hMSC/hAC than that of hMSC culture, especially that as compared to hMSC group, MMP1 expression was 2.9× lower in hAC and 1.8× lower in hMSC/hAC, and MMP3 expression was 5.8× lower in hAC and 2.1× lower in coculture under hypoxia conditions (Figure 5A). We also checked MMP13 expression, which showed a similar expression trend to MMP1 and MMP3 (Figure S5). ELISA results showed that the secreted MMP1 expression gradually decreased along with time in all groups (Figure 5C), and hypoxia dramatically reduced the MMP1 expression from the third week, especially for hAC and coculture groups. Both hAC and hMSC/hAC groups showed much lower secreted MMP1 expression, especially under hypoxia conditions, which

was in good line with the gene expressions of MMP1 and MMP3.

The hypotrophic markers ALPL and COL10A1 are directly involved in the hypertrophy process, and the gene expressions are measured by RT-PCR. The ALP activity was detected by ALP biochemical assay. The expressions of ALPL and COL10A1 were significantly inhibited by hypoxia in hAC and hMSC/hAC groups, which showed dramatically lower expressions of ALPL and COL10A1 than that in the hMSC group (Figure 6A). The ALP activity was hardly detected in the hAC group, while the hMSC group showed relatively high ALP activity (Figure 6B). The ALP activity was reduced significantly by coincubating hMSC/hAC, especially under the hypoxia conditions, which indicated a coculture system of hMSC/hAC could be a promising way to benefit the chondrogenesis of hMSCs and dedifferentiation of chondrocytes. Runt-related transcription factor 2 (RUNX2) is the upstream gene of ALPL and COL10A1 and one important transcription factor in chondrocyte, and it also showed a similar expression trend with ALPL and COL10A1 (Figure S6), demonstrating efficiently repressed hypertrophy and dedifferentiation using cocultured hydrogel systems under hypoxia conditions.

CONCLUSIONS

It is the first demonstration that in situ forming pH-degradable hydrogels as a suitable cell scaffold provide a promising approach to coculturing hMSCs and hACs under hypoxia for autologous chondrocyte implantation. These FDA-approved PVA-based hydrogels showed good biocompatibility with controlled cross-linking density and degradation property. In these hMSC/hACs cocultured hydrogel systems several features have been integrated: (i) they presented good cartilage matrix production, especially under hypoxia; (ii) they significantly repressed the hypertrophy and dedifferentiation; (iii) the most important thing is that they mitigated the disadvantages of single cell type and reduced the required dosage of chondrocytes. Based on this, much more efforts need to be driven into building the optimal chondrogenesis bioenvironments for cartilage tissue engineering.

ASSOCIATED CONTENT

Ⓢ Supporting Information

The Supporting Information is available free of charge on the ACS Publications website at DOI: 10.1021/acs.bio-mac.7b01271.

> ^{1}H NMR spectra of PVA-VEA and PVA-VEA-SH, mesh sizes of PVA hydrogels, cell viability detected by PrestoBlue assay, gene expression of cartilage markers HIF1a, gene expression of catabolic gene MMP13, and gene expression of RUNX2 (PDF).

AUTHOR INFORMATION

Corresponding Authors
*E-mail: w.chen@cpu.edu.cn.
*E-mail: cpuhdc@cpu.edu.cn.

ORCID Ⓞ
Wei Chen: 0000-0003-4017-9722

Author Contributions
‡These authors made equal contributions to this work.

Notes
The authors declare no competing financial interest.

ACKNOWLEDGMENTS

REFERENCES

(1) Huey, D. J.; Hu, J. C.; Athanasiou, K. A. *Science* **2012**, *338*, 917−921.
(2) Madeira, C.; Santhagunam, A.; Salgueiro, J. B.; Cabral, J. M. S. *Trends Biotechnol.* **2015**, *33*, 35−42.
(3) Mollon, B.; Kandel, R.; Chahal, J.; Theodoropoulos, J. *Osteoarthr. Cartilage* **2013**, *21*, 1824−1833.
(4) McAlindon, T. E.; Bannuru, R. R.; Sullivan, M. C.; Arden, N. K.; Berenbaum, F.; Bierma-Zeinstra, S. M.; Hawker, G. A.; Henrotin, Y.; Hunter, D. J.; Kawaguchi, H.; Kwoh, K.; Lohmander, S.; Rannou, F.; Roos, E. M.; Underwood, M. *Osteoarthr. Cartilage* **2014**, *22*, 363−388.
(5) Bugbee, W. D.; Pallante-Kichura, A. L.; Görtz, S.; Amiel, D.; Sah, R. *J. Orthop. Res.* **2016**, *34*, 31−38.
(6) Glyn-Jones, S.; Palmer, A. J. R.; Agricola, R.; Price, A. J.; Vincent, T. L.; Weinans, H.; Carr, A. J. *Lancet* **2015**, *386*, 376−387.
(7) Makris, E. A.; Gomoll, A. H.; Malizos, K. N.; Hu, J. C.; Athanasiou, K. A. *Nat. Rev. Rheumatol.* **2014**, *11*, 21.
(8) Huang, B. J.; Hu, J. C.; Athanasiou, K. A. *Biomaterials* **2016**, *98*, 1−22.
(9) Brittberg, M.; Lindahl, A.; Nilsson, A.; Ohlsson, C.; Isaksson, O.; Peterson, L. *N. Engl. J. Med.* **1994**, *331*, 889−895.
(10) Lam, J.; Lu, S.; Kasper, F. K.; Mikos, A. G. *Adv. Drug Delivery Rev.* **2015**, *84*, 123−134.
(11) Jones, B. A.; Pei, M. *Tissue Eng., Part B* **2012**, *18*, 301−311.
(12) Hubka, K. M.; Dahlin, R. L.; Meretoja, V. V.; Kasper, F. K.; Mikos, A. G. *Tissue Eng., Part B* **2014**, *20*, 641−654.
(13) Pittenger, M. F.; Mackay, A. M.; Beck, S. C.; Jaiswal, R. K.; Douglas, R.; Mosca, J. D.; Moorman, M. A.; Simonetti, D. W.; Craig, S.; Marshak, D. R. *Science* **1999**, *284*, 143−147.
(14) Noeth, U.; Steinert, A. F.; Tuan, R. S. *Nat. Clin. Pract. Rheumatol.* **2008**, *4*, 371−380.
(15) Mak, J.; Jablonski, C. L.; Leonard, C. A.; Dunn, J. F.; Raharjo, E.; Matyas, J. R.; Biernaskie, J.; Krawetz, R. J. *Sci. Rep.* **2016**, *6*, 23076.
(16) Chen, A. K. L.; Reuveny, S.; Oh, S. K. W. *Biotechnol. Adv.* **2013**, *31*, 1032−1046.
(17) Freyria, A.-M.; Mallein-Gerin, F. *Injury-Int. J. Care. Inj.* **2012**, *43*, 259−265.
(18) Puetzer, J. L.; Petitte, J. N.; Loboa, E. G. *Tissue Eng., Part B* **2010**, *16*, 435−444.
(19) Wu, L.; Leijten, J. C. H.; Georgi, N.; Post, J. N.; van Blitterswijk, C. A.; Karperien, M. *Tissue Eng., Part A* **2011**, *17*, 1425−1436.
(20) Cooke, M. E.; Allon, A. A.; Cheng, T.; Kuo, A. C.; Kim, H. T.; Vail, T. P.; Marcucio, R. S.; Schneider, R. A.; Lotz, J. C.; Alliston, T. *Osteoarthr. Cartil.* **2011**, *19*, 1210−1218.
(21) Bian, L.; Zhai, D. Y.; Mauck, R. L.; Burdick, J. A. *Tissue Eng., Part A* **2011**, *17*, 1137−1145.
(22) Zhong, J.; Guo, B.; Xie, J.; Deng, S.; Fu, N.; Lin, S.; Li, G.; Lin, Y.; Cai, X. *Bone Res.* **2016**, *4*, 15036.
(23) Dahlin, R. L.; Kinard, L. A.; Lam, J.; Needham, C. J.; Lu, S.; Kasper, F. K.; Mikos, A. G. *Biomaterials* **2014**, *35*, 7460−7469.
(24) Markway, B. D.; Tan, G.-K.; Brooke, G.; Hudson, J. E.; Cooper-White, J. J.; Doran, M. R. *Cell Transplant.* **2010**, *19*, 29−42.
(25) Maes, C.; Carmeliet, G.; Schipani, E. *Nat. Rev. Rheumatol.* **2012**, *8*, 358−366.
(26) Meretoja, V. V.; Dahlin, R. L.; Wright, S.; Kasper, F. K.; Mikos, A. G. *Biomaterials* **2013**, *34*, 4266−4273.
(27) Gong, T.; Xie, J.; Liao, J.; Zhang, T.; Lin, S.; Lin, Y. *Bone Res.* **2015**, *3*, 15029.
(28) Vo, T. N.; Shah, S. R.; Lu, S.; Tatara, A. M.; Lee, E. J.; Roh, T. T.; Tabata, Y.; Mikos, A. G. *Biomaterials* **2016**, *83*, 1−11.
(29) Xavier, J. R.; Thakur, T.; Desai, P.; Jaiswal, M. K.; Sears, N.; Cosgriff-Hernandez, E.; Kaunas, R.; Gaharwar, A. K. *ACS Nano* **2015**, *9*, 3109−3118.
(30) Ren, K.; He, C.; Xiao, C.; Li, G.; Chen, X. *Biomaterials* **2015**, *51*, 238−249.
(31) Benders, K. E. M.; van Weeren, P. R.; Badylak, S. F.; Saris, D. B. F.; Dhert, W. J. A.; Malda, J. *Trends Biotechnol.* **2013**, *31*, 169−176.
(32) Liao, J.; Tian, T.; Shi, S.; Xie, X.; Ma, Q.; Li, G.; Lin, Y. *Bone Res.* **2017**, *5*, 17018.
(33) Formica, F. A.; Ozturk, E.; Hess, S. C.; Stark, W. J.; Maniura-Weber, K.; Rottmar, M.; Zenobi-Wong, M. *Adv. Healthcare Mater.* **2016**, *5*, 3129−3138.
(34) Wang, T.; Lai, J. H.; Yang, F. *Tissue Eng., Part A* **2016**, *22*, 1348−1356.
(35) Abbadessa, A.; Mouser, V. H. M.; Blokzijl, M. M.; Gawlitta, D.; Dhert, W. J. A.; Hennink, W. E.; Malda, J.; Vermonden, T. *Biomacromolecules* **2016**, *17*, 2137−2147.
(36) Yodmuang, S.; McNamara, S. L.; Nover, A. B.; Mandal, B. B.; Agarwal, M.; Kelly, T.-A. N.; Chao, P.-h. G.; Hung, C.; Kaplan, D. L.; Vunjak-Novakovic, G. *Acta Biomater.* **2015**, *11*, 27−36.

(37) Tian, T.; Liao, J.; Zhou, T.; Lin, S.; Zhang, T.; Shi, S.-R.; Cai, X.; Lin, Y. *ACS Appl. Mater. Interfaces* **2017**, *9*, 30437−30447.

(38) Burnsed, O. A.; Schwartz, Z.; Marchand, K. O.; Hyzy, S. L.; Olivares-Navarrete, R.; Boyan, B. D. *Acta Biomater.* **2016**, *43*, 139−149.

(39) Rackwitz, L.; Djouad, F.; Janjanin, S.; Nöth, U.; Tuan, R. S. *Osteoarthr. Cartilage* **2014**, *22*, 1148−1157.

(40) Zhu, M.; Feng, Q.; Bian, L. *Acta Biomater.* **2014**, *10*, 1333−1340.

(41) Chen, W.; Hou, Y.; Tu, Z.; Gao, L.; Haag, R. *J. Controlled Release* **2017**, *259*, 160−167.

(42) Rubinstein, M.; Colby, R. H. *Polymer Physics*; Oxford University Press: New York, 2003.

(43) Wu, L.; Cai, X.; Dong, H.; Jing, W.; Huang, Y.; Yang, X.; Wu, Y.; Lin, Y. *J. Cell. Mol. Med.* **2010**, *14*, 922−932.

(44) Jin, R.; Hiemstra, C.; Zhong, Z.; Feijen, J. *Biomaterials* **2007**, *28*, 2791−2800.

(45) Wang, R.; Chen, W.; Meng, F.; Cheng, R.; Deng, C.; Feijen, J.; Zhong, Z. *Macromolecules* **2011**, *44*, 6009−6016.

(46) Kang, A.; Park, J.; Ju, J.; Jeong, G. S.; Lee, S.-H. *Biomaterials* **2014**, *35*, 2651−2663.

(47) Egli, R. J.; Bastian, J. D.; Ganz, R.; Hofstetter, W.; Leunig, M. *J. Orthop. Res.* **2008**, *26*, 977−985.

(48) Benya, P. D.; Shaffer, J. D. *Cell* **1982**, *30*, 215−224.

(49) Hong, E.; Reddi, A. H. *Tissue Eng., Part A* **2013**, *19*, 1015−1022.

(50) Babur, B. K.; Ghanavi, P.; Levett, P.; Lott, W. B.; Klein, T.; Cooper-White, J. J.; Crawford, R.; Doran, M. R. *PLoS One* **2013**, *8*, e58865.

(51) Bian, L.; Hou, C.; Tous, E.; Rai, R.; Mauck, R. L.; Burdick, J. A. *Biomaterials* **2013**, *34*, 413−421.

(52) Feng, Q.; Zhu, M.; Wei, K.; Bian, L. *PLoS One* **2014**, *9*, e99587.

(53) Leijten, J. C. H.; Georgi, N.; Wu, L.; van Blitterswijk, C. A.; Karperien, M. *Tissue Eng., Part B* **2013**, *19*, 31−40.